

Composing For Improvisation with Chaotic Oscillators

Mark Havryliv
 Sonic Arts Research Network
 University of Wollongong
 Australia
 mhavryliv@gmail.com

ABSTRACT

This paper describes a novel method for composing and improvisation with real-time chaotic oscillators. Recently discovered algebraically simple nonlinear third-order differential equations are solved and acoustical descriptors relating to their frequency spectrums are determined according to the MPEG-7 specification. A second nonlinearity is then added to these equations: a real-time audio signal. Descriptive properties of the complex behaviour of these equations are then determined as a function of difference tones derived from a Just Intonation scale and the amplitude of the audio signal. By using only the real-time audio signal from live performer/s as an input the causal relationship between acoustic performance gestures and computer output, including any visual or performer-instruction output, is deterministic even if the chaotic behaviours are not.

Keywords

Chaos and Music, Chaotic Dynamics and Oscillators, Differential Equations and Music, Mathematica, Audio Descriptors and MPEG-7

1. INTRODUCTION

Oscillators derived from the dynamics of chaotic systems are an increasingly popular tool for novel audio synthesis. This follows a trend toward a more vigorous engagement with the properties of chaotic and complex systems that is witnessed across all the creative arts. While chaotic systems have been an inspiration for composers since Xenakis it has only recently become possible to digitally calculate dynamic chaotic systems in real-time — without recourse to custom hardware — and use the results of such calculations to control audio synthesis at control and audio rates.

This paper presents a method for using chaotic oscillators as a controlled compositional and improvisational component; our chaotic oscillators are driven not only by the internal dynamics of their respective equations but the real-time audio input from one or many performers. This takes advantage of the fact that a certain class of chaotic systems, Sprott's third-order 'jerk' functions [15], necessarily include a nonlinear component in order to function as chaotic attractors.

Permission to make digital or hard copies of all or part of this work for personal or classroom use is granted without fee provided that copies are not made or distributed for profit or commercial advantage and that copies bear this notice and the full citation on the first page. To copy otherwise, to republish, to post on servers or to redistribute to lists, requires prior specific permission and/or a fee.

NIME2010, 15–18th June 2010 Sydney, Australia
 Copyright 2010, Copyright remains with the author(s).

Our experimental work indicates that an additional non-linear external driving force at a low frequency does not terminally disrupt the chaotic system's trajectory and indeed can alter perceptually significant characteristics of an oscillator's behaviour. A subset of MPEG-7 audio descriptors are used to categorise firstly a chaotic system's natural behaviours and then its response to external input. Low frequency *difference tones* derived from a Just Intonation scale are used as the external driving input.

This approach is motivated by the conceptual tidiness of a performer's audio driving a complex system with great potential for generating rich behaviour over time that can be displayed acoustically or visually, and used in myriad other ways such as real-time score-generation or data-mining. Further, the techniques described in §3 on audio descriptors, like the spectral mean, spectral flatness and inharmonicity are themselves useful data sources for use in other parts of performance, like visualisation. And, as the mathematics of the systems described here are relatively simple, they can be implemented in several popular real-time synthesis environments.

1.1 Chaos and Aesthetics

The attractiveness of chaos is easy to see, literally. Chaotic patterns and their multitudinous representations are the standard visual trope for the expression of beauty and elegance in mathematics. Artists and researchers are attracted to the complex but recurring patterns and look to deploy the patterns or the dynamics behind them to aesthetic ends.

Sprott himself, a doyen of chaotic analysis and whose third-order differential equations are the focus of this paper, recognised the creative potential in chaos and co-conducted empirical studies into aesthetic preferences for different types of chaotic patterns in 1996 [1]. This was limited to visual representations. In the same year, Dabby published her work on chaotic mappings as a method for musical variation of existing works by Bach, Chopin, Gershwin and others [6]. Variations were generated by mapping a series of pitches from the original work to the chaotic trajectory of one of the three dynamic variables in Lorenz's classic chaotic equation set [11]:

$$\begin{aligned}\dot{x} &= \sigma(y - x) \\ \dot{y} &= x(\rho - z) - y \\ \dot{z} &= xy - \beta z\end{aligned}\tag{1}$$

with the Lorenz parameters $\rho = 28$, $\sigma = 10$ and $\beta = 8/3$ which lead to the classic 'butterfly' image shown in Figure 1, constructed by plotting one dynamic variable against another over time. The musicality and soundness of the results were subjectively validated by musicians familiar with the respective composers, however Dabby warns that considerable energy is required to intelligently manage mappings. In a phrase that could be applied to any novel method of mu-

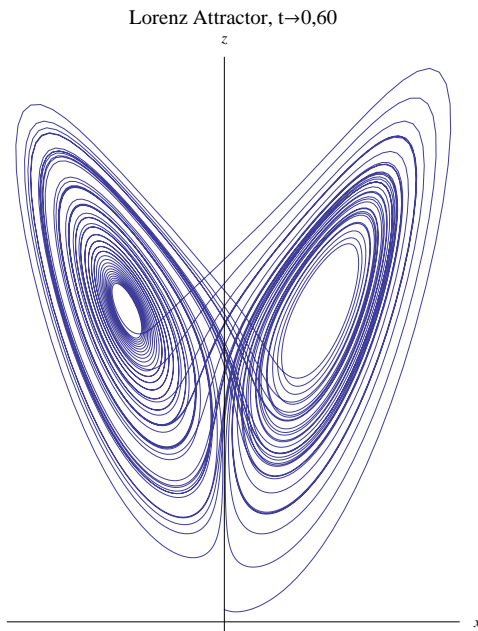


Figure 1: Classic Lorenz attractor parametric plot of $z(t)$ against $x(t)$; initial values $x(0) = 0, y(0) = 1, z(0) = 1.05$.

sic creation, she says: “[t]hough the method will not flatter fools, it can lead explorers into landscapes where, amidst the familiar, variation and mutation allow wild things to grow.”

1.2 Chaos and Audio Synthesis

1.2.1 Granular and FM Synthesis

A 2005 review of works which broaden the scope of musical applications of chaotic patterns is presented by Buraston and Edmonds [4]. This review focuses on chaotic systems expressed as Cellular Automata (CA) and tracks the evolution of musical applications based on the standard visualisations of CA to the various granular synthesis algorithms and complex filters which engage CA’s chaotic dynamics in much more thorough ways and avoid what Peter Bowcott is quoted as referring to as merely “a representation of the visual output” [2]. However, they do note the dominance of software in the MIDI domain and further observe that CA music made with MIDI software tends to concentrate on pitch and duration mappings to the visual representations.

An important article on the use of chaotic systems for audio synthesis is Slater’s 1998 publication [14] in which he uses analogue synthesisers, the 100 and 200 series Buchla Oscillators, to generate chaotic synthesis by creating closed loops between the inputs and outputs of a series of voltage controlled oscillators. More recently, Pinot has implemented many of Slater’s ideas digitally using CSound [13]; Pinot’s *crossfm* family of opcodes demonstrate that personal computers and open-source software are capable of calculating these closed-loop chaotic dynamics for synthesis.

1.2.2 Differential Equations

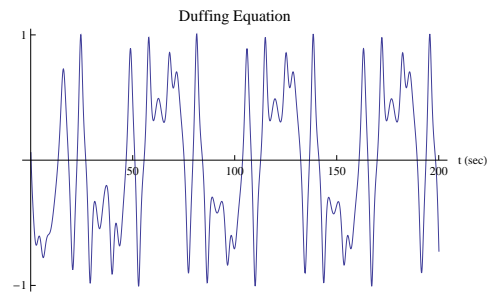
Of more immediate relevance to our work, however, is the 2003 paper in which Yadegari published a method for generating control and audio signals from ordinary differential equations which exhibit chaotic behaviour; he also developed an external object, the *fexpr~* object for Pd,

Max/MSP and jMax, that facilitates the numerical solution of the equations in real-time [17]. In his paper, Yadegari demonstrates the abilities of the object by solving the Duffing equation [9]:

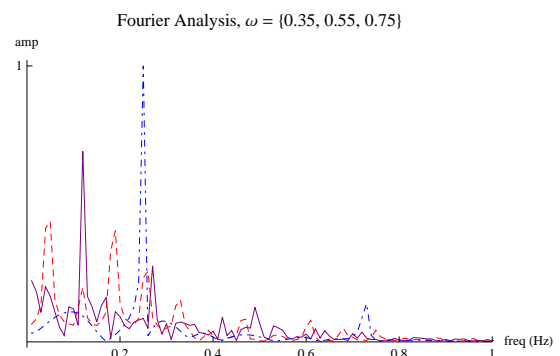
$$\ddot{x} + \delta\dot{x} + \alpha x + \beta x^3 = \gamma \cos(\omega t + \phi) \quad (2)$$

which is a nonlinear second-order differential equation that exhibits chaotic behaviour. This equation derives its nonlinearity from the cubed x^3 term and the constant-frequency cosine driving force; without this driving force the system quickly stabilises from an initial perturbation.

An interesting feature of this system from the perspective of the musician is its high sensitivity to changes in the frequency of the driving cosine.



(a) Duffing oscillator with $\omega = 0.7$ rad/sec.



(b) Fourier analysis of Duffing oscillator with changing ω , line = 0.35, dashed = 0.55 and dash-dotted = 0.75.

Figure 2: Oscillation and spectrum of Duffing equation with $\delta = 0.3, \alpha = -1, \beta = 1, \gamma = 0.5$ and $\phi = 0$.

From Figure 2 we see that changes over a very small range of frequency values for the cosine function produce quite large changes in the frequency spectrum of the resulting Duffing oscillator; indeed, that is the point of chaos! Small changes in initial conditions generate large differences in trajectory over time. Obviously the dominant frequencies in the spectrums shown here lie significantly below the threshold for being perceived as a continuous tone, some manipulation of solving step-size and multiples of the sampling rate is required to raise these frequencies into the audible spectrum.

Another pleasing thing to note is the relatively strong peak for $\omega = 0.75$ rad/sec at approximately 0.25 Hz, and the regular spacing of peaks for $\omega = 0.55$ rad/sec. This suggests that simply using the series of $x(t)$ values may with no manipulation lead to tonally useful oscillations, belying the typical characterisation of chaotic oscillators as merely coloured noise. The ‘tonality coefficient’ is one of the MPEG-7 audio descriptors and we use it to measure the tonal content of some chaotic equations more explicitly in §3.

Through experimentation the upper limit for possible driving frequencies was found to be approximately 1.6 rad/sec; frequencies above this were unable to overcome the system's natural inertia. The upper limit can be raised, though, by altering other initial variables. Also, this frequency limit is only the case while the Duffing oscillation period remains as shown in Figure 2(b), that is, well below 1 Hz. As the oscillator is sampled such that its dominant frequencies enter, the audible spectrum the upper limit for ω will also increase.

2. AUDIO INPUT TO CHAOTIC EQUATIONS

2.1 Just Intonation

This relatively low limit brings to mind the naturally-occurring difference tones, or *beatings*, associated with Just Intonation music which occur between closely-spaced intervals; the amplitude envelope of the resultant signal is dominated by these low-frequency difference tones and seems an excellent candidate for a real-time driving signal to replace the constant cosine term in Eq. 2.

Managing and creating difference tones is a large part of Just Intonation composition and improvisation, and in strongly harmonic instruments like the marimba the potential for deliberate and perceivable difference tones is high when scale intervals are well-chosen. The rate of beating is determined by the difference in frequency between adjacent scale degrees,¹ and at low frequencies is perceived as a constant frequency amplitude envelope rather than an additional tone.

Just Intonation scales are devised by combining intervals that can be represented by whole-number frequency ratios taken from the harmonic series that describe a distance from an arbitrary fundamental tone [7]. The scale used in this paper is a 12-note Meta Slendro scale based on Erv Wilson's interpretations of Pascal's Triangle, or *Mt. Meru*, to which percussionist Kraig Grady² has tuned his marimba [8].

Table 1: Meta Slendro scale intervals, harmonic ratios, an octave of frequencies and distance from equal temperament scale.

Degree	Ratio	Freq. (Hz)	Cents from ET
0	1/1	352	F +13.7
1	65/64	357.5	F +40.5
2	9/8	396	G +17.6
3	37/32	407	G# -35
4	151/128	415.25	G# -0.2
5	21/16	462	A# -15.5
6	43/32	473	A# +25.2
7	3/2	528	C +15.6
8	49/32	539	C# -48.7
9	25/16	550	C# -13.7
10	7/4	616	D# -17.5
11	57/32	627	D# +13.2

Listed in Table 1, the scale is seen to have six opportunities for generating difference tones below 12 Hz between adjacent scale degrees which is well below the threshold for the perception of a continuous tone.

12 Hz is somewhat high for use with the Duffing equation, though we need not be limited by that. In 2000,

¹In instruments with strong harmonics separate beating also occurs between harmonics other than the fundamental.

²A collaborator of the author's.

Table 2: List of Sprott's jerk equations used in this paper.

System	$\{x(0), \dot{x}(0), \ddot{x}(0)\}$
1 : $\ddot{x} = -2.017\dot{x} + \dot{x}^2 \pm x$	$\{0, 0, \pm 1\}$
2 : $\ddot{x} = -0.5\dot{x} - \dot{x} - x + \text{sgn}(x)$	$\{0, 1, 0\}$
3 : $\ddot{x} = -0.6\dot{x} + 2.8\dot{x} - \dot{x}^3 - x$	$\{0, 1, 0\}$

Sprott published 22 third-order differential equations which he classes as the simplest quadratic jerk³ function that produces chaos; most of the equations have only three terms [15].

These equations are attractive because of their algebraic and computational simplicity; in the same paper, Sprott designs simple analogue circuits based on the earlier Chua's circuit [5]. They are also simpler to solve computationally because we only need to evaluate the derivative of one function rather than the three in the Lorenz attractor.

2.2 Sprott's Jerk Functions

Of the 22 equations, we have selected a subset principally on the aesthetics of their parametric plots, and then by looking for interesting natural harmonic spectra. The following parametric plots are created from the equations in Table 2. They were solved for $t \rightarrow 0, 250$ using the *Mathematica* numerical differential equation solver, *NDSolve* with a maximum step size of 0.01.

As the equations are solved over time, we record the time-series values for the respective derivatives. The parametric plots are then drawn by plotting the time-series values of either $x(t)$, $\dot{x}(t)$ or $\ddot{x}(t)$ against each other, and they demonstrate that so simple a decision as which derivatives are plotted against each other can lead to significantly different results. As seen here, a general rule of thumb is that the second derivative $\ddot{x}(t)$ plotted against $x(t)$ produce figures with sharper turns, particularly if the nonlinearity in the system is coupled to the x term as it is in the second system where the Figure 3(d) features what resembles a skewed square shape centred about the origin.

It is outside the scope of this paper to head deeply into the mathematical properties of these equations but I urge the interested reader to Sprott's excellent book [16] for more information.

3. AUDIO DESCRIPTORS

Now we have the time-series values for $x(t)$, $\dot{x}(t)$ and $\ddot{x}(t)$ we can apply some form of acoustic analysis. The first obvious step is to perform Fourier transforms on the respective time-series and observe their frequency content. Figure 4 shows the natural frequency spectrum for the time-series $x(t)$ over 0.25 seconds.

This figure in itself is quite useful; one clearly sees the peaks at 84, 168 and 248 Hz and gets a sense of the signal-to-noise ratio. We can go further, though, by employing the audio descriptors now implemented in the MPEG-7 specification which, among other descriptors, calculate the signal's spectral centroid, spectral spread, spectral flatness and tonality, fundamental frequency (f_0) and inharmonicity [10]. The following is a brief summary of these descriptors, and their implementations in *Mathematica* are available for free download on the author's website.⁴ *Mathematica* code was developed to take advantage of its powerful numerical

³Jerk is the 3rd time derivative of position x , after velocity \dot{x} , and acceleration \ddot{x} .

⁴<http://www.uow.edu.au/~mh675/mathematica>

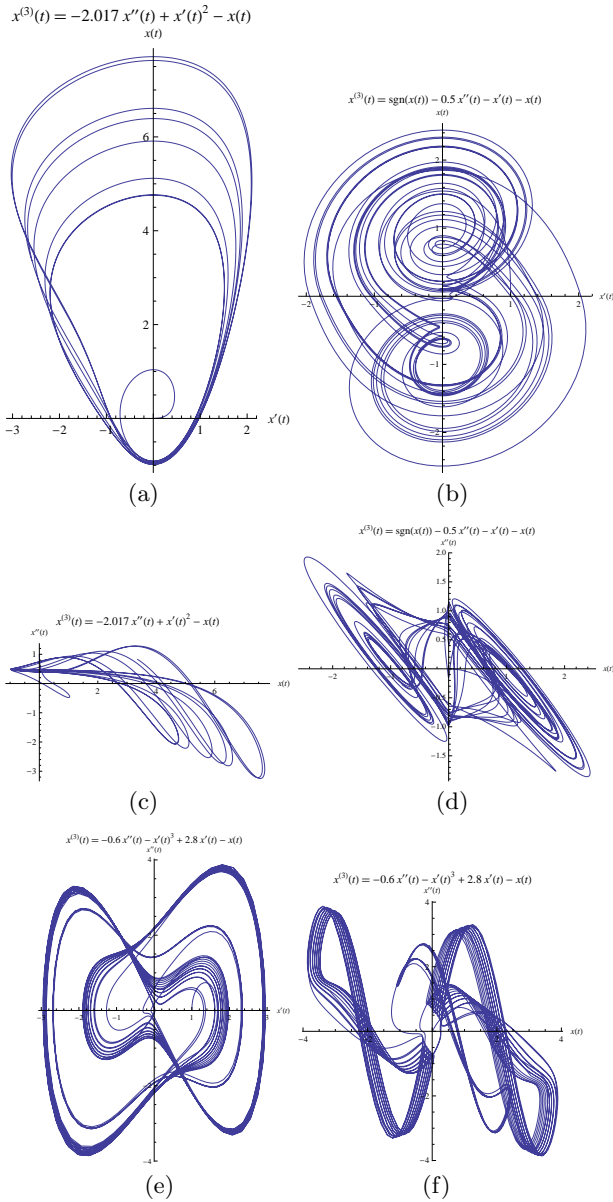


Figure 3: Spratt’s equations from Table 2 plotted parametrically.

differential equation solvers, statistical analysis and graphing abilities.

The following descriptions are taken from Peeters [12] and reverse-engineered code from the Matlab implementation⁵. For real-time use, Bullock [3] has released libxtract, a library for real-time audio feature extraction in Pd, Max/MSP and SuperCollider 3.

3.1 Spectral Descriptors

This subsection mathematically describes some of the simpler descriptors, and provides real values for these and a few other descriptors the author has found useful for the frequency distribution in Figure 4.

3.1.1 Spectral Centroid

The spectral centroid μ is the centre of mass of the spectrum, where the continuous sum of frequency components multiplied by their amplitudes is divided by the sum of all

⁵Available at <http://mpeg7.doc.gold.ac.uk/>.

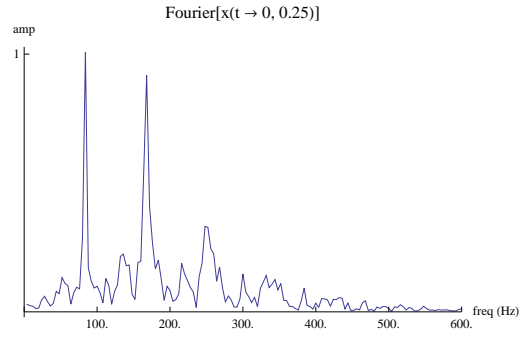


Figure 4: Spectrum for $x(t)$ of system 1.

amplitudes. Combined with the spectral spread, this value is a useful shorthand for spectral concentration.

$$\mu = \int x \cdot p(x) \delta x \quad (3)$$

with

$$x = \text{freq}(x)$$

$$p(x) = \frac{\text{amp}(x)}{\sum_x \text{amp}(x)} \quad (4)$$

The spectral centroid for Figure 4 is 159 Hz.

3.1.2 Spectral Spread

The spectral spread is calculated as the variance of the distribution around the centroid.

$$\sigma^2 = \int (x - \mu)^2 \cdot p(x) \delta x \quad (5)$$

The spectral spread for Figure 4 is 98 Hz, or 0.618 of the centroid.

3.1.3 Spectral Flatness/Tonality Coefficient

The spectral flatness is a measure of the noisiness of a signal and is also used to determine a ‘tonality co-efficient’. For tonal signals, the spectral flatness is close to 0 and for noisy signals it is close to 1, while the opposite is true of the tonality coefficient. The spectral flatness is given by:

$$\text{SFM} = \frac{1}{N} \frac{\left(\prod_{n=1}^N \text{amp}(n) \right)^{1/N}}{\sum_{n=1}^N \text{amp}(n)}, \quad (6)$$

and the tonality coefficient is given by:

$$\text{tonality} = \min \left(\frac{10 \cdot \log_{10}(\text{SFM})}{-60}, 1 \right) \quad (7)$$

The spectral flatness for Figure 4 is 0.1221 and the tonality coefficient is 0.1522; note that the log function in the conversion from SFM to tonality means the measure of tonality drops rapidly with even a small value for the signal’s noisiness.

3.1.4 Fundamental Frequency

The fundamental frequency is defined as the frequency whose integer multiple best explains the content of the signal spectrum. This means in some cases a ‘missing fundamental’ is computed because it explains existing harmonic peaks better than the lowest peak. Such is the case with

the calculation of f_0 for the above spectrum, for which the function returns 42.49 Hz.

Since it is difficult to assume a ‘sensible’ harmonic content for a chaotic system this value is usually not particularly useful on its own, however, it is useful in determining the next feature: inharmonicity.

3.1.5 Inharmonicity

Inharmonicity describes the divergence of spectral peaks from a signal that would be constituted of only exact multiples of f_0 . It is determined by comparing and summing the spectral distance between would-be harmonic peaks and actual spectral peaks multiplied by the energy content of that spectral peak, then dividing by the total energy of the spectral peaks. An inharmonicity value of 0 indicates a purely harmonic signal and a value of 1, an inharmonic signal. Once the fundamental frequency is determined, inharmonicity is calculated as:

$$\text{inharmonicity} = \frac{2}{f_0} \frac{\sum_h |f(h) - h * f_0| * a^2(h)}{\sum_h a^2(h)} \quad (8)$$

where $f(h)$ and $a(h)$ are the frequency and amplitude of the spectral peaks. This algorithm gives an inharmonicity value for our signal of 0.046, which is very harmonic and observable from the spacing of the spectral peaks in Figure 4.

4. AUDIO INPUT — RESULTS

The following graphs show the influence of the beating tones generated by intervals in Table 1 on a time-series signal for $x(t)$ generated from the first chaotic system in Table 2 as analysed by the audio descriptor methods just discussed.

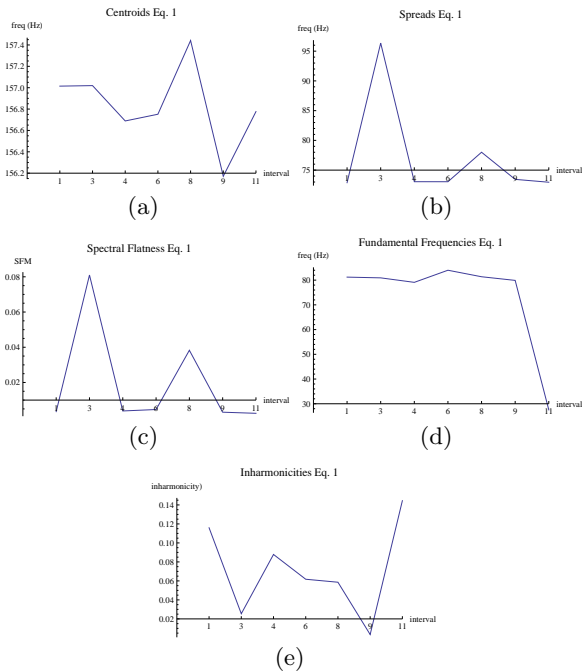


Figure 5: Graphs of audio descriptor outputs for chaotic system 1 with driving inputs.

In each case a simple model of a marimba tone:

$$\text{sig}(t) = 0.3 \sin(2\pi * ft) + 0.2 \sin(2\pi * 2ft) \quad (9)$$

was summed with an adjacent frequency for the intervals in the scale where the difference tone was less than 12 Hz.

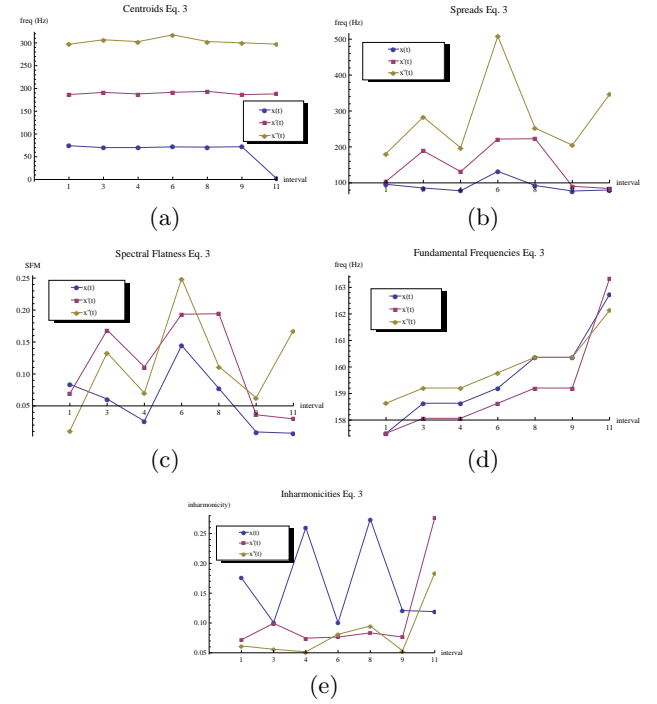


Figure 6: Audio descriptor outputs for chaotic system 3 with each of the three dynamic variables, $x(t)$, $\dot{x}(t)$ and $\ddot{x}(t)$.

5. CONCLUSION

The response of the chaotic oscillator for system 1 (Figure 5) is shown to change in response to different audio inputs and these changes are within the bounds of perceptual significance, particularly spectral flatness and inharmonicity. An interesting result comes from the observation that the difference tones for the final three intervals are equal; some descriptors are clearly more sensitive to the low frequency beatings than they are to the actual frequency of the tones.

Figure 7 demonstrates the sensitivity of the spectral flatness measure to the amplitude of the driving signal. Meanwhile, the plots in Figure 6 which display the response of $x(t)$ and its two derivatives indicate that although most descriptors are different there are difference tones that produce very similar results; from a compositional perspective these moments would be useful as pivot points.

6. ACKNOWLEDGEMENTS

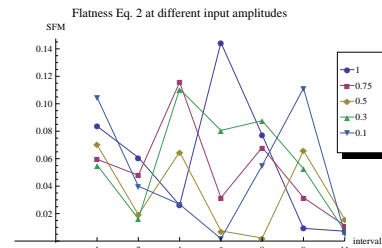


Figure 7: Change in spectral flatness for $x(t)$ in system 2 as a function of interval and amplitude of audio driving signal (1 = max).

The author would like to thank Kraig Grady for inspiring research worthy of his musicality, Warren Burt for introducing me to Sprott's jerk functions, Eva Cheng for her timely advice in regards to the field of audio descriptors and Greg Schiemer for his continued demonstration of the potential in Just Intonation.

7. REFERENCES

- [1] D. J. Aks and J. C. Sprott. Quantifying aesthetic preference for chaotic patterns. *Journal of the International Association of Empirical Studies of the Arts*, 14(1):1–16, 1996.
- [2] P. Bowcott. Cellular automata as a means of high level control of granular synthesis. In *Proceedings of the 1989 International Computer Music Conference*, 1989.
- [3] J. Bullock. Libxtract: A lightweight library for audio feature extraction. In *Proceedings of International Computer Music Conference*, 2007.
- [4] D. Burraston and E. Edmonds. Cellular automata in generative electronic music and sonic art: Historical and technical review. *Digital Creativity*, 16(3):165–185, 2005.
- [5] L. O. Chua and F. Ayrom. Designing non-linear single op-amp circuits: A cookbook approach. *International Journal of Circuit Theory Applications*, 13:235–268, 1985.
- [6] D. S. Dabby. Musical variations from a chaotic mapping. *CHAOS*, 6:95–107, 1996.
- [7] D. B. Doty. *The Just Intonation Primer: An Introduction to the Theory and Practice of Just Intonation*. The Just Intonation Network, 3rd edition, 2002.
- [8] K. Grady. An introduction to the scale of mt. meru and other recurrent sequence scales. <http://www.anaphoria.com/wilsonintroMERU.html>, Accessed: February, 2010.
- [9] D. W. Jordan and P. Smith. *Nonlinear Ordinary Differential Equations*. Clarendon Press, New York, 2nd edition, 1987.
- [10] T. Lindsay, I. Burnett, S. Quackenbush, and M. Jackson. Fundamentals of audio descriptors. In B. Manjunath, P. Salembier, and T. Sikora, editors, *Introduction to MPEG-7 Multimedia Content Description Interface*. Wiley & Sons, 2002.
- [11] E. N. Lorenz. Deterministic nonperiodic flow. *Journal of Atmospheric Science*, 20:130–141, 1963.
- [12] G. Peeters. A large set of audio features for sound description (similarity and classification) in the cuicado project. Technical report, IRCAM, Analysis/Synthesis Team, 2004.
- [13] F. Pinot. Cross frequency modulation. *CSound Journal*, 12, 2009.
- [14] D. Slater. Chaotic sound synthesis. *Computer Music Journal*, 22(2):12–19, 1998.
- [15] J. Sprott. Simple chaotic systems and circuits. *American Journal of Physics*, 68:758–763, 2000.
- [16] J. C. Sprott. *Chaos and Time-series Analysis*. Oxford University Press, 2003.
- [17] S. Yadegari. Chaotic signal synthesis with real-time control: Solving differential equations in pd, max/msp and jmax. In *Proceedings of the 6th International Conference on Digital Audio Effects*, 2003.